



SPM studies of ferroelectric nanostructures prepared by a microemulsion-assisted method onto substrates[#]

Maria Torres^{1,*}, M. Lourdes Calzada¹, Brian Rodriguez², Marin Alexe³, Lorena Pardo¹

¹*Instituto de Ciencia de Materiales de Madrid, CSIC. C/ Sor Juana Inés de la Cruz, 3, Cantoblanco, 28049 Madrid, Spain*

²*Conway Institute of Biomolecular and Biomedical Research, University College Dublin, Belfield, Dublin 4, Republic of Ireland*

³*Max Planck Institute of Microstructure Physics, Weinberg 2, D-06120 Halle, Germany*

Received 30 March 2009; received in revised form 22 August 2009; accepted 16 September 2009

Abstract

Ferroelectric PbTiO₃ nanostructures have been fabricated using two different procedures that involve microemulsions and Chemical Solution Deposition onto Pt/TiO₂/SiO₂/(100)Si substrates. The first procedure enables the fabrication of structures with controlled size and shape, as observed by Atomic Force Microscopy (AFM) topography and computer assisted quantitative analysis, while the second procedure, in addition, yields very small (≈ 20 nm) isolated, ferroelectric nanoislands. The ferroelectric character of the nanostructures is demonstrated using Piezoelectric Force Microscopy (PFM). The ferroelectric properties depend on the height of the nanostructures, showing a strong pinning layer effect for the smaller ones, revealed by the asymmetry of the piezoelectric hysteresis loops.

Keywords: *Microemulsion, Ferroelectric, Nanoparticles, SPM*

I. Introduction

Recently, significant effort has been directed into the development of ultra-high density non-volatile ferroelectric random access memories (NV Fe-RAMs) based on ordered arrays of ferroelectric nanostructures [1–3].

This approach requires the fabrication of an array of ferroelectric nanostructures of equal size and shape onto the substrate. The methods described in the literature to obtain such structures can be divided into the so-called top-down methods (based on etching a thin or ultrathin film) [3] and the bottom-up approaches (based on building up the structures from the bottom) [2].

If surfactant molecules are added to an emulsion (mixture of two immiscible liquids), they try to organize in order to minimize the chemical potential, stabilizing the groups of one of the phases in the other and preventing them from reverting into two different lay-

ers [4]. Emulsions are usually described as water-in-oil and oil-in-water type or direct and inverse emulsions, respectively, depending on which is the continuous medium. The shape and size of the colloidal aggregates depend on the type of surfactant and the nature and relative quantity of the two phases present in the emulsion. One of these possible assemblies are micelles. Micelles are a grouping of surfactant molecules where either the hydrophobic (in a polar continuous phase) or the hydrophilic (in a non-polar continuous phase) ends cluster inward to escape the continuous phase, keeping one of the liquids of the emulsion inside. If the heads from the inside of the aggregate, then it is called an inverse micelle and in the opposite case, it is called a direct micelle. Micelles are formed by the core, a liquid pool inside, and the shell, formed by the surfactant.

The microemulsion formed by reverse micelles can include at the pool not only water but nanodrops of a different nature [5–7]. In this case, the micelles also play the role of nanoreactors and the mixture formed is called a micellar solution. Controlling the amount of water to surfactant involved, it is possible to control the micelle size and, consequently, the nanoparticle size.

[#]Paper presented at 6th COST 539 Workshop, *Advance Functional Characterization of Nanostructured Materials*, February 23–25, 2009, ICMC-CSIC, Madrid, Spain

* Corresponding author: tel: +34 913 349-000
fax: +34 91 372 0623, e-mail: mtorres@icmm.csic.es

Although the microemulsion method is a well-known procedure for the preparation of nanopowders [5–7], it has been rarely used in the case of ferroelectrics grown on substrates, whether in thin film form [8–10] or isolated nanostructures [11].

Chemical Solution Deposition (CSD) techniques provide a good stoichiometry control at relatively low-cost for the fabrication of ferroelectric perovskite oxide thin films [12]. And so, the procedures here described involve both microemulsions and CSD.

Nanostructures present the challenge of measuring and characterizing systems that are below the limit of the resolution of conventional microelectronics technology. Scanning Probe Microscopies (SPMs) are a group of techniques that enable the characterization of nano-ferroelectric materials at a local scale. By PFM, the so called size limit of ferroelectricity was determined to be 20 nm [13] as it was found as the size from which a ferro-piezoresponse could not be measured by this technique. However, PFM depends not only on the electromechanical response of the nanostructures, but also on the entire measurement device and sample system, including the type of cantilever used, its mechanical characteristic and the interface between sample and substrate [14].

Here, we present the SPM characterization of ferroelectric nanoparticles, prepared by two microemulsion assisted methods, onto polycrystalline Pt/TiO₂/SiO₂/(100)Si substrates.

II. Experimental

Microemulsions, sol and micellar solutions are prepared as described elsewhere [15,16]. Deposition of the microemulsions and the micellar solutions onto the Pt/TiO₂/SiO₂/(100)Si substrates was carried out by spin-coating at 2000 rpm for 45 s, following two different procedures: the first one was to coat the substrates with the micellar solutions. Drying and crystallization was made according to the procedure described elsewhere [15]. This is denoted process A. The second procedure consists of the spin-coating of the microemulsion and, onto this emulsion layer; the micellar solution was spun-coated, dried and crystallized in the same conditions used for process A. This is denoted process B.

A commercial Scanning Force Microscopy (SFM) by Nanotec was used to study the surface topography of the PbTiO₃ nanostructures. The tips used for topographic measurements (Atomic Force Microscopy, AFM) were Si cantilevers (force constant 42 N/m, resonance frequency 320 kHz).

All SEM investigations were performed with a JEOL 7500F scanning electron microscope operated at 3 kV on the samples, without using any conductive coating layer.

Particle size distributions were calculated using MIP software by Digital Image Systems from AFM and SEM images. Here the size of the nanostructures can be well defined by the equivalent diameter to their circular shape, since they have more or less the same dimensions in all

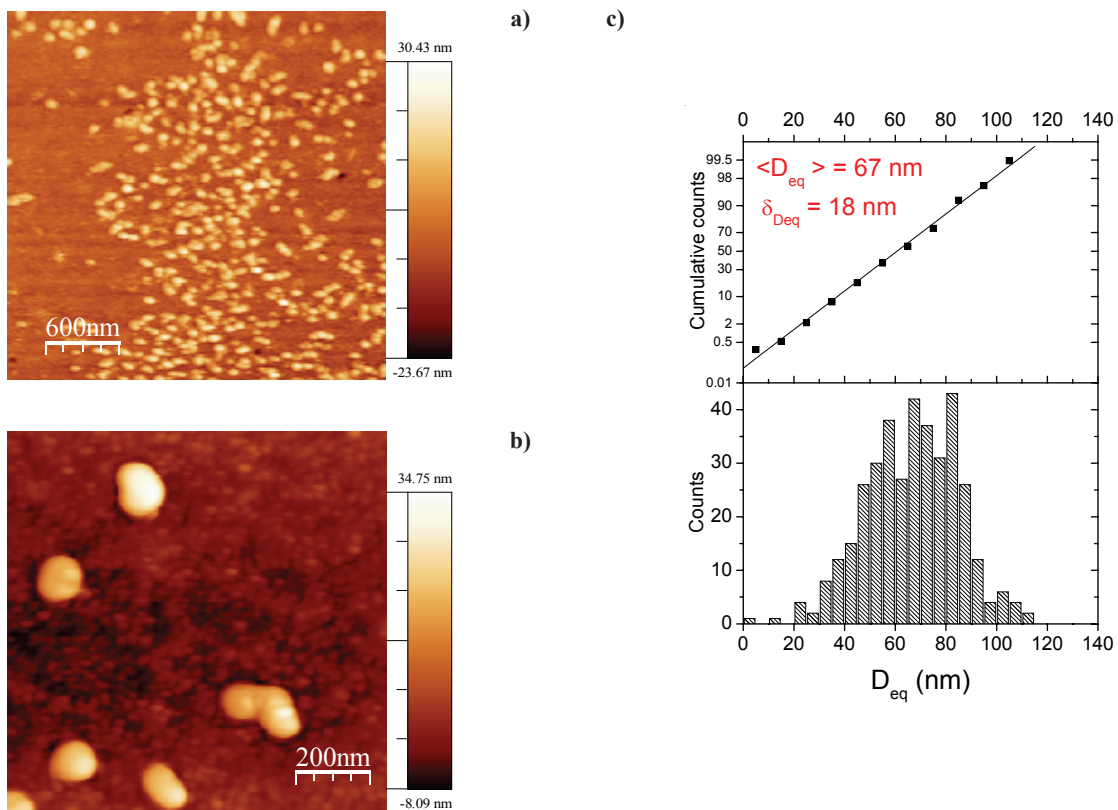


Figure 1. AFM images of the particles prepared by procedure A (a-b), and their corresponding size distribution and probabilistic plot (c)

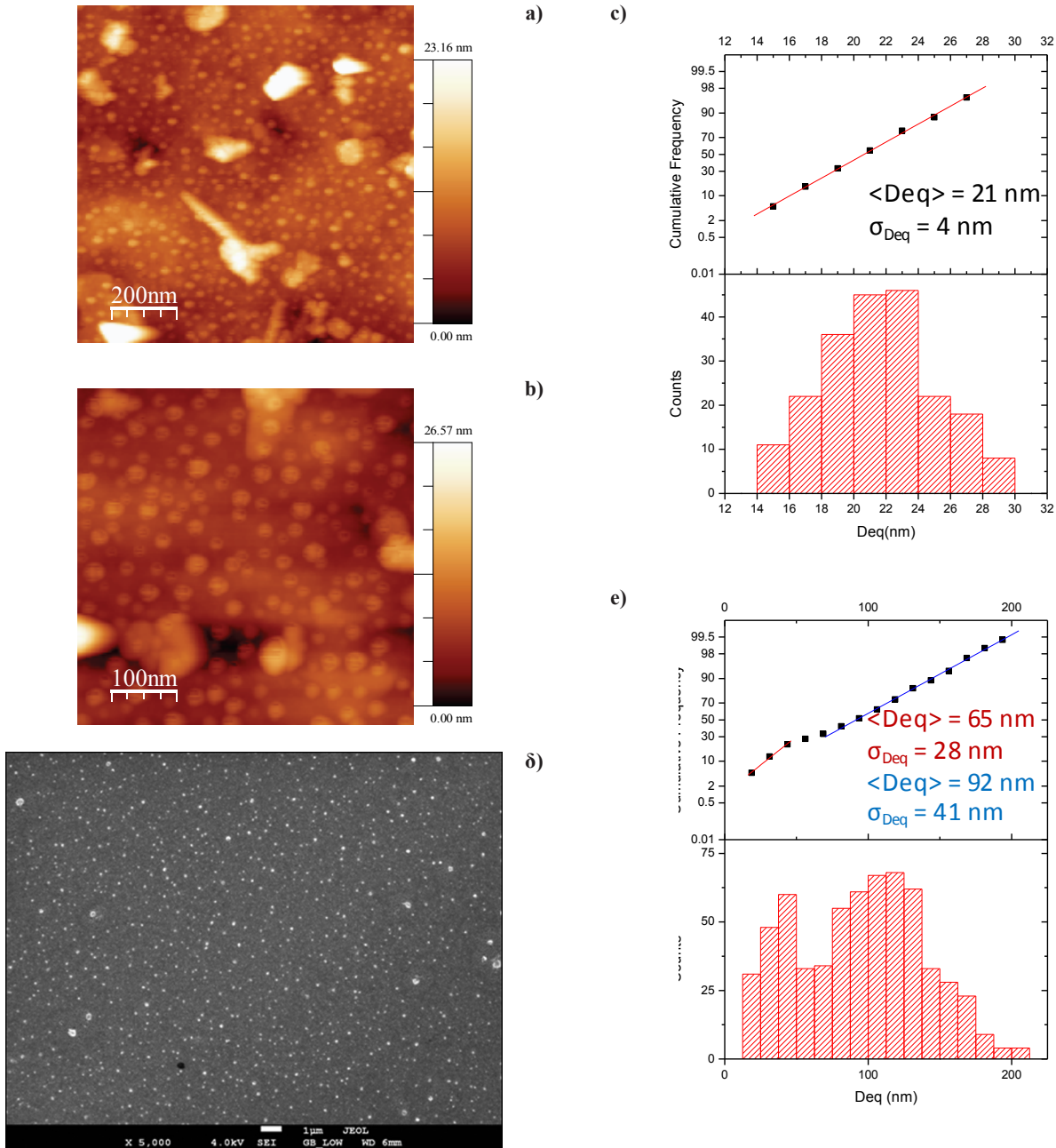


Figure 2. AFM images of the particles prepared by procedure B (a-b), and the size distribution of the isolated particles and probabilistic plot (c). The corresponding SEM image (d) and the size distribution of the aggregates and their probabilistic plot (e)

directions. To calculate the average value of the measured distributions of equivalent diameter, $\langle D_{eq} \rangle$, and their standard deviation, σ_{Deq} , the fitting of the line obtained at the probability plot of such distribution was used [17].

For local piezoelectric activity measurements (Piezoresponse Force Microscopy, PFM), two kinds of probes were used, both Pt/Ir coated Si cantilevers (force constant 42 N/m and 5 N/m, resonance frequency 320 kHz and 65 kHz, respectively). Out-of-field or hysteresis loops were measured. They are obtained when inducing piezoelectric vibration in the nanostructures under increasing and decreasing (DC) voltage, measuring when the field is driven back to zero [18].

III. Results

Fig. 1a,b show AFM topography images of the isolated nanostructures obtained by procedure A. The nanostructures have a homogeneous size and shape as demonstrated by the size distribution plotted in Fig. 1c. However, these structures seem to be formed by agglomeration of smaller particles because they are not perfectly rounded but show some smaller distortion. The size distribution of the nanoislands is a single Gaussian distribution with an average equivalent diameter, $\langle D_{eq} \rangle$, of 67 nm and a standard deviation, σ_{Deq} , of 18 nm. The height of the particles is estimated as 20 nm from AFM topography line scans.

In the case of the nanostructures prepared by the procedure B, AFM images (Fig. 2a,b) show rounded small isolated particles and larger structures formed by the agglomeration of the smaller ones. The size distribution is also a single Gaussian one, characterized by an average size, $\langle D_{eq} \rangle$, of 21 nm and a standard deviation, σ_{Deg} , of 4 nm. Height of the particles is estimated as 6 nm from line scans of the AFM images.

The SEM image (Fig. 2d) of the same sample at smaller magnification shows bright spots. The size distribution of these spots is a bimodal distribution of average sizes, $\langle D_{eq} \rangle$, 65 nm and 92 nm and standard deviations, σ_{Deg} , of 28 nm and 41 nm, respectively, as shown in Fig. 2e.

The ferroelectric response of these nanostructures was proved by measuring local piezoelectric hysteresis loops by PFM as well as by the obtained PFM images of phase and amplitude. Fig. 3b,c shows the piezoresponse images of some isolated nanostructures prepared by procedure A, which topography image is shown in Fig. 3a. Fig. 3e,f represents the piezoresponse of those prepared by method B, which topography image is shown in Fig. 3d.

Fig. 4a shows the plot of an out-of-field hysteresis loop of an isolated nanoparticle of ~ 83 nm of lateral size prepared by procedure A. Fig. 4b shows a hystere-

sis loop corresponding to a nanoparticle of ~ 36 nm of diameter prepared by procedure B.

IV. Discussion

Procedure A results into nanostructures with a narrow distribution of size and homogeneous shape. It is assumed that the micelles are acting as nanoreactors, preventing nanoparticles from agglomerating before the crystallization. However, when we compare nanoparticles from the same micellar solution and processed by methods A and B, we can see that process B leads to smaller particles. We can understand these as the result of defects that the polycrystalline Pt substrate presents (roughness ± 17 nm with some pores present), and because of this, the deposited micelles in process A tend to concentrate in those points, leading to a slight agglomeration of the primary nanoparticles after the thermal treatment, when all the surfactant is eliminated. This can be observed at the high magnification image (Fig. 1b), where some of the A processed nanostructures show an imperfect spherical shape that would correspond to the merged primary particles.

Therefore, nanostructures prepared by procedure A are agglomerated themselves as explained before. Their average size is similar to the one of the bright spots at the SEM image in Fig. 2d. We can think that these spots

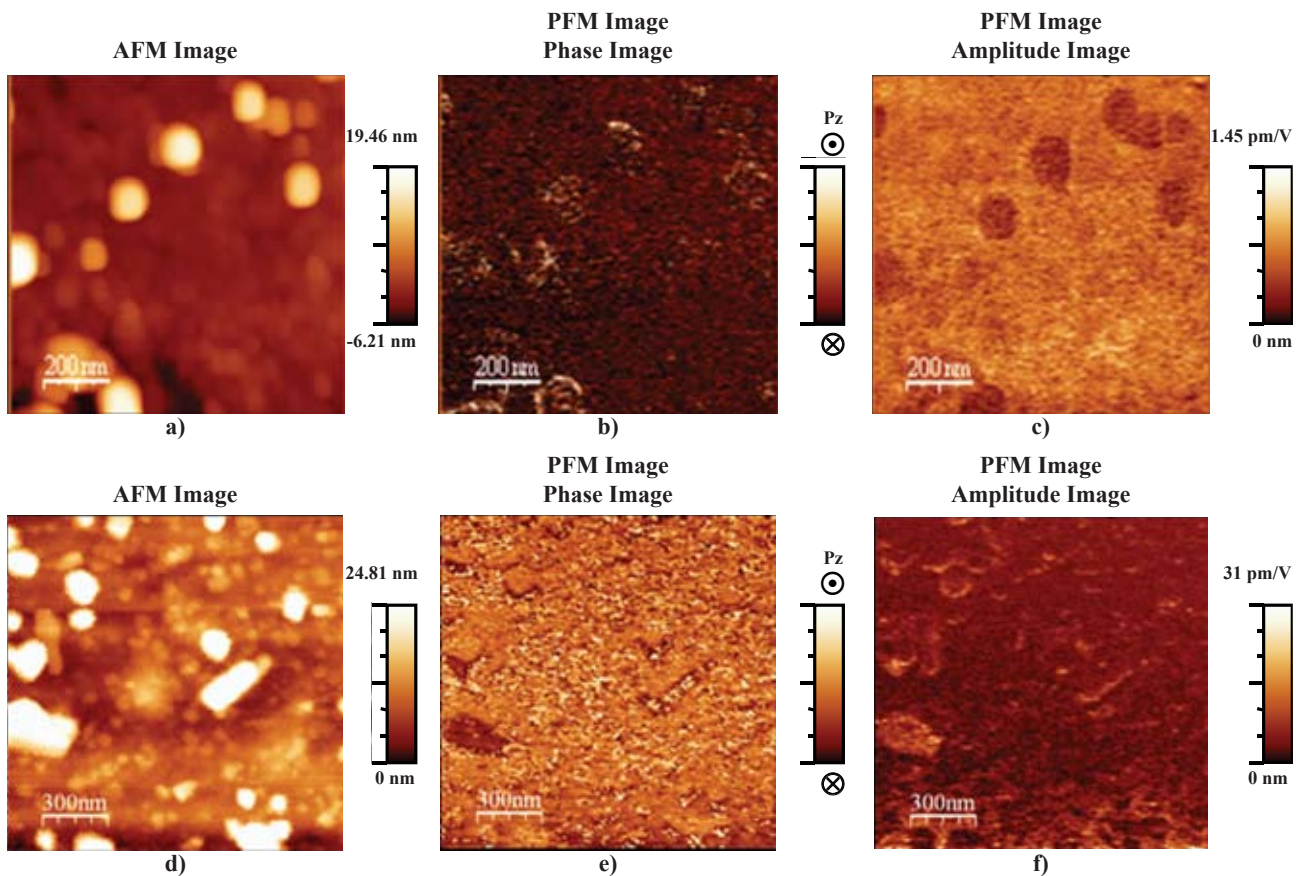


Figure 3. PFM images of phase and amplitude and their corresponding topography images of particles obtained by procedure A (a-d) and procedure B (e-f)

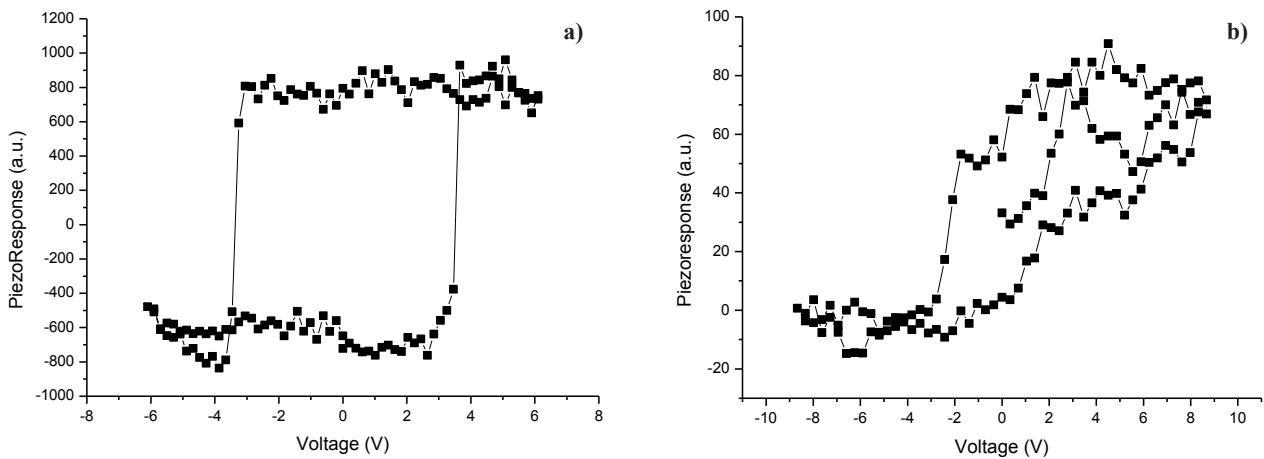


Figure 4. Out-of-field hysteresis loops obtained by PFM on isolated nanoparticles fabricated by procedure A (a) and procedure B (b)

are the agglomerates that can be seen at the AFM images (Fig. 2a,b) corresponding to the sample prepared by procedure B. Thus, some primary particles still agglomerate, as in process A, even in larger agglomerates. However, we observe that this effect is partially eliminated when the substrate is pre-treated with a microemulsion layer in process B, resulting into a smoother substrate surface. This can be easily observed by comparing AFM images taken at the same magnification and shown in Fig. 1b and Fig. 2a.

The microemulsion layer used provides a functionalized surface onto which the micellar solution is more uniformly deposited. Thus, the agglomeration of the nanoparticles is minimized. This procedure is a well-known one for polymer films or ultrathin films [19] and, to the best of our knowledge, it is the first time that is used in combination with microemulsion mediated synthesis, applied to ferroelectric oxides.

In addition, the ferro-piezoelectric responses that particles prepared by both methods are different. In contrast to nanostructures prepared by procedure A, where the hysteresis loop is symmetric with respect to the piezoresponse and electric voltage axis, nanoparticles prepared by procedure B are not. Asymmetry with respect to electric voltage axis effect is well-known as imprint phenomena taking place in most thin films [20]. In ferroelectric nanoparticles of ~ 100 nm, asymmetry with respect to piezoresponse axis was previously found [14] and attributed to a pinned layer at the bottom part of the nanostructure that clamps the switching of the polarization. The nature of the pinned layer is unknown, but most probably related with certain crystal structure defects occurring at the interface between the substrate and the ferroelectric particle. When the field is established in the same direction as the pinned polarization, its contribution adds to that switched by the field, whereas when the field is applied in the opposite polarity, this contribution is subtracted from the switched one, giving place to the asym-

metry of the loop. This effect is not observed for the sample prepared by procedure A. One could think that the pinning layer effect is increased when decreasing the nanostructures size. Since this layer is an intrinsic characteristic of the interface between nanostructure and substrate, its effect is proportional to the ratio between interface volume, of some few unit cells height, and whole volume of the nanoparticle. Consequently, it should be larger in nanostructures from procedure B, smaller in lateral size, but also in height (6 nm) compared with the height of nanostructures from procedure A (20 nm).

V. Conclusions

Isolated single particles of PbTiO_3 are prepared by two different methods that involve microemulsion mediated synthesis and Chemical Solution Deposition onto $\text{Pt/TiO}_2/\text{SiO}_2/(100)\text{Si}$ substrates. These procedures results in nanostructures with a controlled shape and size. Nanoparticles fabricated by both procedures have a Gaussian distribution of their size with an average value of 21 nm – primary particles in procedure B - and 67 nm – in procedure A - and a narrow distribution of size. In addition, procedure B is proved as an effective way of controlling deagglomeration of the nanostructures. Their ferro-piezoelectric behavior had been proved by PFM, showing different ferroelectric behavior depending on the height of the nanostructures: smaller ones show a strong pinning of the layer corresponding to the interface between the nanostructure and the substrate.

Acknowledgement: This work has been financed by the Spanish Project MAT2007-61409. M. Torres thanks to the Spanish Ministry of Science and Innovation for supporting her Ph. D. grant of the FPI program as well as for the financial support of her short-stay at the Max-Planck-Institut für Mikrostrukturphysik at Halle. Authors would also like to thank the support of MIND NoE (contract CE FP6 515757-2).

References

1. J.F. Scott, “New developments on FRAMs: [3D] structures and all-perovskite FETs”, *Mater. Sci. Eng. B-Solid*, **120** (2005) 6–12.
2. Y.S. Cho, K. Fujimoto, Y. Hiranaga, Y. Wagatsuma, A. Onoe, K. Terabe and K. Kitamura, “Tbit/inch(2) ferroelectric data storage based on scanning nonlinear dielectric microscopy”, *Appl. Phys. Lett.*, **81** (2002) 4401–4403.
3. S.H. Ahn, W.W. Jung and S.K. Choi, “Size dependence of initial polarization direction in nanosized epitaxial PbTiO_3 islands fabricated by hydrothermal epitaxy below Curie temperature”, *Appl. Phys. Lett.*, **86** (2005) 172901.1–172901.3.
4. H. Wennerstrom and B. Lindman, “Micelles – physical-chemistry of surfactant association”, *Phys. Rep.-Rev. Section of Phys. Lett.*, **52** [1] (1979) 1–86.
5. M.P. Pileni, “The role of soft colloidal templates in controlling the size and shape of inorganic nanocrystals”, *Nat. Mater.*, **2** (2003) 145–150.
6. M. Perez, N. Zambrano, M. Ramirez, E. Tyrode and J.L. Salager, “Surfactant-oil-water systems near the affinity inversion. XII. Emulsion drop size versus formulation and composition”, *J. Disper. Sci. Technol.*, **23** (2002) 55–63.
7. H. Herrig and R. Hempelmann, “A colloidal approach to nanometre-sized mixed oxide ceramic powders”, *Mater. Lett.*, **27** (1996) 287–292.
8. J.H. Kim and F.F. Lange, “Seeded epitaxial growth of PbTiO_3 thin films on (001) LaAlO_3 using the chemical solution deposition method”, *J. Mater. Res.*, **14** (1999) 1626–1633.
9. S.S. Kim, E.K. Choi, J.K. Kim, J.S. Kim, T.K. Song and J. Kim, “Effects of surfactant on surface morphology and orientation of Nb-doped $\text{Bi}_4\text{Ti}_3\text{O}_{12}$ thin films”, *J. Korean Phys. Soc.*, **42** (2003) S1126–S1129.
10. T. Schneller, “Wet Chemical deposition of BaTiO_3 nanopowders in mesoscopic layers”, p. 241, in: *Book of Abstracts of Electroceramics X*, Toledo, 2006.
11. S. Bhattacharyya, S. Chattopadhyay and M. Alexe, “Fabrication of isolated ferroelectric nanostructures”, *Mater. Res. Soc. Symp. Proceed.*, **740** (2003) I10.13.11–I10.13.16.
12. R.W. Schwartz, T. Schneller and R. Waser, “Chemical solution deposition of electronic oxide films”, *Comptes Rendus Chimie*, **7** (2004) 433–461.
13. A. Roelofs, T. Schneller, K. Szot and R. Waser, “Piezoresponse force microscopy of lead titanate nanograins possibly reaching the limit of ferroelectricity”, *Appl. Phys. Lett.*, **81** (2002) 5231–5233.
14. B.J. Rodriguez, S. Jesse, M. Alexe and S. V. Kalinin, “Spatially resolved mapping of polarization switching behavior in nanoscale ferroelectrics”, *Adv. Mater.*, **20** (2008) 102–114.
15. M.L. Calzada, M. Torres, L.E. Fuentes-Cobas, A. Mehta, J. Ricote and L. Pardo, “Ferroelectric self-assembled PbTiO_3 perovskite nanostructures onto (100) SrTiO_3 substrates from a novel microemulsion aided sol-gel preparation method”, *Nanotechnol.*, **18** (2007) 375603–375610.
16. N.J. Phillips, M.L. Calzada and S.J. Milne, “Sol gel-derived lead titanate films”, *J. Non-Cryst. Solids*, **147** (1992) 285–290.
17. J. Ricote and L. Pardo, “Microstructure-properties relationships in samarium modified lead titanate piezoceramics: 1. Quantitative study of the microstructure”, *Acta Mater.*, **44** (1996) 1155–1167.
18. C. Harnagea. “Local piezoelectric response and domain structures in ferroelectric thin films investigated by voltage-modulated force microscopy”, *Ph.D. Thesis*, Halle, 2001.
19. G. Decher, “Layered nanoarchitectures via directed assembly of anionic and cationic molecules”. pp: 507–528 in *Comprehensive Supramolecular Chemistry - Vol 9*. Eds. by J-P. Sauvage and M. Wais. Pergamon, Oxford, 1996.
20. H.N. AlShareef, D. Dimos, W.L. Warren and B.A. Tuttle, “Voltage offsets and imprint mechanism in $\text{SrBi}_2\text{Ta}_2\text{O}_9$ thin films”, *J. Appl. Phys.*, **80** (1996) 4573–4577.